



Circum-Antarctic warming events between 4 and 3.5 Ma recorded in marine sediments from the Prydz Bay (ODP Leg 188) and the Antarctic Peninsula (ODP Leg 178) margins

C. Escutia ^{a,*}, M.A. Bárcena ^b, R.G. Lucchi ^c, O. Romero ^a, A.M. Ballegeer ^b, J.J. Gonzalez ^a, D.M. Harwood ^d

^a Instituto Andaluz de Ciencias de la Tierra, CSIC-Universidad de Granada, Fuentenueva s/n, 18002-Granada, Spain

^b Universidad de Salamanca, Departamento de Geología, 37008 Salamanca, Spain

^c GRC Geociències Marines, Departament d'Estratigrafia, P. i Geociències Marines, Universitat de Barcelona, Facultat de Geologia C/ Martí i Franquès, s/n, 08028-Barcelona, Spain

^d Department of Geosciences, University of Nebraska-Lincoln, P.O. Box 880340, Lincoln, NE 68588-0340, USA

ARTICLE INFO

Article history:

Received 25 March 2009

Accepted 22 September 2009

Available online 4 October 2009

Keywords:

early-middle Pliocene
glaciomarine sedimentation
Antarctic Peninsula
Prydz Bay
circum-Antarctic
glacial–interglacial cycles

ABSTRACT

Our study characterizes glacial and interglacial deposition on two Antarctic margins in order to discriminate between regional and continent-wide early to middle Pliocene warm intervals that caused sea-ice reduction and continental ice sheet retreat. We use a multi-proxy (i.e., sediment facies and grain size, siliceous microfossils, biogenic opal, geochemical composition and clay mineralogy) approach to examine sediments recovered in drill holes from the West Antarctic Peninsula and the East Antarctic Prydz Bay margins, focusing on the climatic record between 4 and 3.5 Ma.

Warm conditions in both East and West Antarctica are recorded, which based on our age model correspond to periods of prolonged or extreme warmth correlated with isotopic stages Gi5, Gi1, MG11 and MG7. For the Gi5 interglacial our data corroborates the 60% *Dictyocha* percentage at 34.60 mbsf previously reported from Prydz Bay and interpreted to indicate a SSST of about 5.6 °C above present. Our higher-resolution sampling interval shows *Dictyocha* percentages up to 87.5%, suggesting even higher SSSTs above present levels. During MG11, which coincides with the section dated by the magnetic polarity reversal Gilbert-Gauss at 3.58 Ma, SSSTs were tentatively 2.5°–4° warmer than present, and reduced sea-ice cover in Prydz Bay and probably also west of the Antarctic Peninsula is indicated by increased primary productivity. In addition, a reduction of ice sheet size is suggested by the bioturbated and IRD-enriched facies that characterize these high-productivity intervals. Based in our age model and calculated sedimentation rates glacial–interglacial cyclicity between 4 and 3.5 Ma in the cores from Antarctic Peninsula and Prydz Bay Sites, result in frequencies consistent with obliquity and precession forcing.

The prolonged early-middle Pliocene warm period was superimposed on a cooling trend recorded by the: 1) increase of the terrigenous sediment supply at all our sites starting between 3.7 and 3.6 Ma, and 2) decrease in SSSTs (from >5.6 °C at 3.7 Ma to 4°–2.7 °C at 3.6 Ma, and 2.5 °C at 3.5 Ma.) indicated by the silicoflagellate W/C R from Site 1165. We postulate that, although the start of a cooling trend is recorded at about 3.7–3.6-Ma, relatively warm conditions prevailed until 3.5 Ma capable of maintained open marine conditions with reduced or no sea-ice and reduced ice sheet volume and extent.

The information in this paper regarding the timing of continental-wide and regional warm events and the paleoenvironmental conditions that characterized them (i.e., SSST, extent of sea ice, and ice sheet size) are relevant to help constrain paleoclimate and ice sheet models for the early-middle Pliocene, a time period when the level of warming according to the Intergovernmental Panel on Climate Change 2007 report, is within range of the estimates of the Earth's global temperature increases for the 21st century. These data, when linked to modeling studies like those of Pollard and DeConto (2009) will further our understanding of how these ice sheets may respond to future warming of the southern high latitudes.

© 2009 Elsevier B.V. All rights reserved.

1. Introduction

During the Pliocene Epoch, between 5 and 3 million years (Ma), the Earth experienced higher global surface temperatures than today (about 3 °C) (Sloan et al., 1996; Dowsett et al., 1996; Haywood et al., 2000) and higher atmospheric CO₂ concentrations than pre-industrial

* Corresponding author.

E-mail addresses: cescutia@ugr.es (C. Escutia), mbarcena@usal.es (M.A. Bárcena), rglucchi@ub.edu (R.G. Lucchi), oromero@ugr.es (O. Romero), amballeger@usal.es (A.M. Ballegeer), jhonjairo@ugr.es (J.J. Gonzalez), dharwood1@unl.edu (D.M. Harwood).

times (Raymo et al., 1996). Warming during the early Pliocene, culminating in the mid-Pliocene Climatic Optimum at about 3 Ma is suggested by the marine oxygen isotopic record obtained in low and high-latitude regions (e.g., Hodell and Venz, 1992; Kennett and Hodell, 1995; Shackleton et al., 1995; Zachos et al., 2001; Lisiecki and Raymo, 2005). Obliquity-driven oscillations (41 ka) in the $\delta^{18}\text{O}$ signal of benthic foraminifera with amplitudes of up to 0.6‰, which dominate the Pliocene period, are capable of producing up to 30 m sea-level changes, but have been considered insufficient to give evidence for large scale Antarctic Ice Sheet deglaciation because uncertainties about the temperature changes in the deep-ocean (Shackleton et al., 1995). What is known about climate cycles and changes in ice-sheet volume during the early-middle Pliocene, however, is mostly derived from oxygen isotopic records from low and mid latitudes and from sea-level curves derived from low latitude passive continental margins. Proximal sediment records from the Antarctic margin are critical for deciphering of how past extreme periods of warmth and cold have affected sea-ice extent and Antarctic ice sheet volume and extent.

Results from drilling around the Antarctic margin during the past twenty years (e.g., Ocean Drilling Program-ODP Legs 178 in the Antarctic Peninsula and 119 and 188 in Prydz Bay; Cape Roberts and ANDRILL Programs in the Ross Sea) are providing valuable insights with regard to Antarctic Ice Sheet dynamics since its inception around 34 Ma. For the early to mid Pliocene these records show that the Southern Ocean has experienced higher temperatures (e.g., Bohaty and Harwood, 1998) and the Antarctic Ice Sheet has had a dynamic behavior (e.g., Webb and Harwood, 1991; Haywood et al., 2009). For example, ODP Leg 188 records obtained from the East Antarctic Prydz Bay continental shelf show evidence of repeated advance and retreat of the Lambert ice stream across the shelf in the Late Miocene and through the early Pliocene (Hambrey et al., 1991; Passchier et al., 2003; O'Brien et al., 2004). Juntilla et al. (2005) pointed out that fluctuations of smectite and chlorite within the clay mineral assemblage at Site 1165, on the Prydz Bay continental rise, during the middle Pliocene are consistent with a dynamic behaviour of the East Antarctic Ice Sheet (EAIS). Diatom assemblages recovered from Prydz Bay ODP sites 1166 and 1165, suggest low sea-ice concentrations through much of the Pliocene (Whitehead et al., 2005). In addition, silicoflagellate assemblages from Site 1165 pinpoint three intervals (4.6–4.8 Ma, 4.3–4.4 Ma, and 3.7 Ma) within the Pliocene, when Southern Ocean SSTs were about 5 °C warmer than today (Whitehead and Bohaty, 2003). These data are consistent with isotopic estimates of warmer conditions than present during the Early Pliocene (Hodell and Venz, 1992). In addition, three periods of enhanced sediment supply originating from East Antarctica are recognized in the Late Miocene–Pliocene record of the East Kerguelen Ridge sediment drift, in the Indian Ocean to the north of Prydz Bay (Joseph et al., 2002). These pulses in sediment accumulation were interpreted as result of periodically warmer, less stable, ice sheet conditions during this time. On land, a warm Pliocene was inferred from an 8 m-thick sequence of early Pliocene diatomaceous sands and silts exposed at Marine Plain in the Vestfold Hills (Pickard et al., 1988; Harwood et al., 2000; Whitehead et al., 2001). These deposits were interpreted to indicate that the ice margin was about 50 km further inland and no floating ice was covering the site.

Climate cycles have also been reported from West Antarctica. For example, in the western Antarctic Peninsula continental rise sediments recovered during ODP 178 confirmed that ice streams repeatedly advanced to the shelf break throughout the Pliocene (Barker et al., 2002; Hillenbrand and Ehrmann, 2005; Hepp et al., 2006). Based on sediment physical and geochemical properties from ODP Site 1095 in the Antarctic Peninsula, Hepp et al. (2006) propose a highly dynamic Antarctic Peninsula Ice Sheet (APIS) that is sensitive to Milankovitch eccentricity forcing during the early Pliocene. Periodic APIS reduction is suggested to explain the increased terrigenous flux to the continental rise

corresponding to maximum amplitudes in the elements Fe and K (Hepp et al., 2006). The sedimentary section recovered from the Ross Sea by the ANDRILL program at Site AND-1B contains a well-dated record of cyclic variations in the ice sheet extent that are obliquity-paced (Naish et al., 2009). This record shows the West Antarctic Ice Sheet (WAIS) collapsed repeatedly in the Ross Sea embayment during interglacial periods characterized by high surface water productivity and minimal summer sea ice and air temperatures above freezing (Naish et al., 2009).

A strong decrease in sea-ice coverage at both, the Antarctic Peninsula and the East Antarctic margin starting at 5.3 Ma and maintained during the early Pliocene is indicated by opal deposition (Grützner et al., 2005; Hillenbrand and Ehrmann, 2005; Hepp et al., 2006). A reduced extent of sea-ice in the Southern Ocean is indicated by an increase in biological productivity during the early Pliocene that is shown by the increase in opal deposition rates at East Antarctic ODP Site 1165 and West Antarctic Site 1095 (Hillenbrand and Fütterer, 2002; Grützner et al., 2005; Hillenbrand and Ehrmann, 2005).

Although evidence for a warm early Pliocene is constructed from different sites around Antarctica, little is known about the timing and extent of an East and West Antarctic Ice Sheet response to these warmer oceanographic conditions. These data are necessary to provide constraints to paleoclimate models that can help in forecasting future ice sheet behavior. In this paper we study and compare the sedimentary record from two Antarctic continental margins, one draining the APIS off the Pacific margin of the Antarctic Peninsula and the other draining the EAIS off Prydz Bay (Figs. 1 and 2). Our main objective is to characterize glacial and interglacial deposition at each margin, and to discriminate between regional and continent-wide early to middle Pliocene warm intervals that can cause sea-ice and continental ice sheet retreat. We conducted a high-resolution and multi-proxy (i.e., sediment facies and grain size, siliceous microfossils, biogenic opal, geochemical composition and clay mineralogy) analysis of sediments deposited between 4 and 3.5 Ma. Our results indicate open marine conditions with warm SSTs, reduced sea ice and significant reduction of both the APIS and the EAIS during the early and middle warm periods of the Pliocene.

2. Oceanographic setting

The structure and circulation of water masses that overlie the western Antarctic Peninsula continental shelf are mainly controlled by the Antarctic Circumpolar Current (ACC), and especially by its narrowness at the proximity of the Drake Passage (Orsi et al., 1995). Two oceanographic fronts are located directly west of the Antarctic Peninsula, the Polar Front in the north and the southern boundary of the ACC in the south (Orsi et al., 1995). Sites 1095 and 1096 (Western Antarctic Peninsula) (Fig. 1), are covered by a thin surface layer of cold water of about 100–150 m water depth (Smith et al., 1999), the Antarctic Surface Water (AASW). This water mass has a temperature range from –1.8 to 1.0 °C and a salinity range from 33.0 to 33.7‰. Surface water currents on the shelf west of the Antarctic Peninsula show weak cyclonic gyres (Smith et al., 1999). In the Pacific sector of the Southern Ocean off the Antarctic Peninsula, the Circumpolar Deep Water (CDW) represents a mixture of North Atlantic Deep Water (NADW) and recirculated waters from the Indian and Pacific Oceans (Patterson and Whitworth, 1990). Thus, below the AASW there is a warmer and more saline water mass, the Circumpolar Deep Water (CDW) with temperatures around 1.6 °C, which protrudes onto the shelf (Hofmann et al., 1996; Smith et al., 1999). The CDW provides a consistent deep source of heat and salt and low oxygen water for the Western Antarctic Peninsula (Smith et al., 1999).

Site 1165 is located within or near a large cyclonic gyre, known as the Antarctic Divergence (AD), between 60°E and 100°E (Fig. 2). The AD results from the confluence of two currents: the ACC, which flows clock-wise around Antarctica, and the Polar Current (PC), which flows

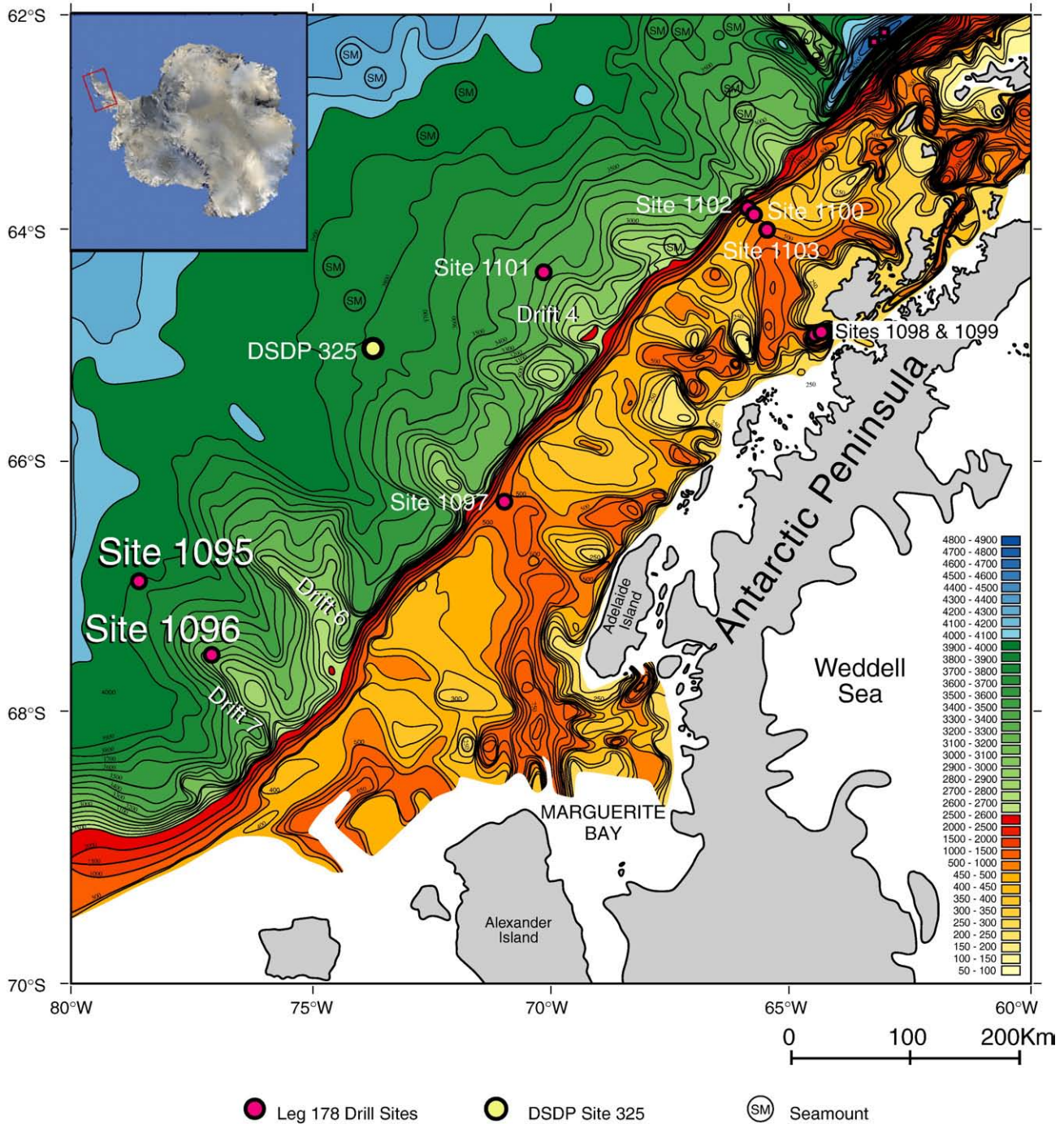


Fig. 1. Map showing the location of the ODP Sites 1095 and 1096 on the continental rise Drift 7 located on the Pacific margin of the Antarctic Peninsula.

westward (counter-clock-wise) close to the continent (Smith et al., 1984). Deep-water circulation is controlled by the influx of NADW, which transports warmer, saltier and nutrient-rich water from the North Atlantic as a consequence of the thermohaline circulation. When the NADW reaches the Southern Ocean it forms the CDW Water. The NADW, or the vertically mixed CDW, circulates onto the Prydz Bay shelf delivering nutrients and heat, which causes sea-ice to melt. In contrast to the western Antarctic Peninsula shelf, Prydz Bay is an area of saline bottom water formation, the Prydz Bay Bottom Water, a precursor of Antarctic Bottom Water (Nunes and Lennon, 1996).

At present, the climatic conditions at Site 1165 are characterized by cold SST; average SSST is 0.5 °C, average winter SST is −1.8 °C and

mean annual SST is approximately −0.5 °C (Gordon and Molinelli, 1982). Winter sea-ice distribution shows a monthly median extent up to 59°S, with sea-ice free conditions during summer (National Snow and Ice Data Center, NISDC).

3. Materials and methods

3.1. Core locations

The sediment cores analyzed for this study were collected by the Ocean Drilling Program (ODP) Leg 178 west of the Antarctic Peninsula (Sites 1095 and 1096) and Leg 188 in Prydz Bay (Site 1165, Figs. 1 and 2). Sites 1095 and 1096 were drilled on a hemipelagic sediment

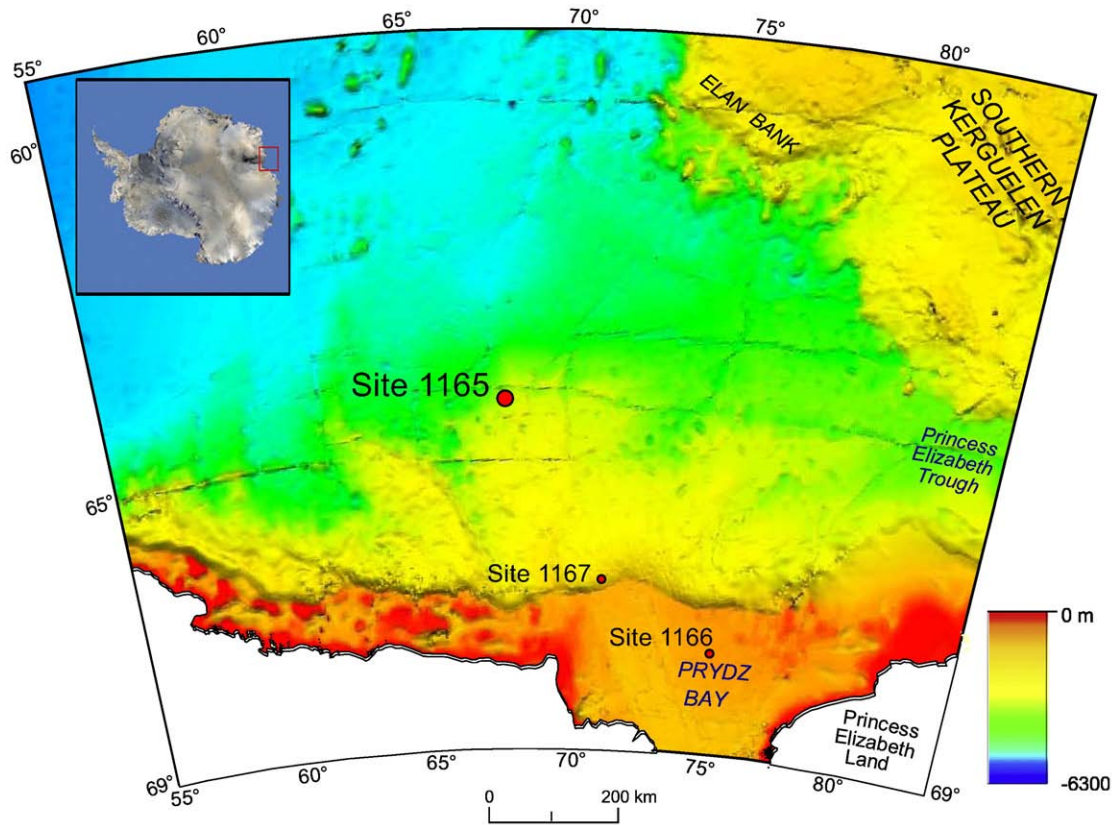


Fig. 2. Map showing the location of the ODP Site 1165 located on the continental rise Wild Drift off Prydz Bay.

drift (Drift 7, [Rebescio et al., 1997](#)) on the continental rise ([Barker et al., 1999](#)). These two sites were chosen in order to verify the proximal (1096) and distal (1095) sedimentary response to climatic variability affecting the APIS. Site 1095 is located at $66^{\circ} 59' S$ and $78^{\circ} 29' W$, at 3840 m water depth and it was cored with the advanced piston corer (APC) to 483.3 meters below sea floor (mbsf) ([Barker et al., 1999](#)). For this study we focused on a 10 m interval from 95.50 to 105.50 mbsf. Site 1096 is located at $67^{\circ} 34' S$ and $76^{\circ} 57' W$, at 3153 m water depth and was drilled using an Extended Core Barrel (XCB) coring tool ([Barker et al., 1999](#)). For our study we focused on a 7.5-meter interval from 401 to 408.5 mbsf.

Site 1165 was drilled into the Wild Drift located at $64^{\circ} 22.78' S$ and $67^{\circ} 13.14' E$, in 3537 m water depth on the continental rise offshore from Prydz Bay ([O'Brien et al., 2001](#)). This site was selected in order to obtain a proximal record of the response of the EAIS to glacial/interglacial cycles that could be compared with the Leg 178 sites. Site 1165 was cored with the APC to 147.9 mbsf. This paper focuses on the 6 m long interval recovered from 34 to 40 mbsf.

3.2. Core description and grain size analyses

Sediment cores were re-described during a visit to the IODP-Bremen Core Repository (BCR). The visual description focused on sedimentary structures and texture, colour changes, with a preliminary compositional investigation through smear slides. In addition, selected intervals were X-radiographed at a medical facility in Bremen for detailed analyses on sedimentary facies and structures.

The textural characteristics of sediments were determined using both wet sieving at $63 \mu m$ to separate the sand from mud (silt and clay) fractions, and the particle size analyser Sedigraph (SedigraphIII 5120) to analyze the fine fraction between 63 and $0.68 \mu m$ with a resolution of $1/4 \phi$ and using a sodium metaphosphate dispersant solution of 0.05% to avoid particle flocculation. The sediment grain

size was classified according to the scale of [Freedman and Sanders \(1978\)](#).

In addition, we used the Magnetic Susceptibility (MST) data sets produced during the ODP Legs ([Barker et al., 1999](#); [O'Brien et al., 2001](#)), which are available from the ODP database (<http://www-odp.tamu.edu/database/>).

3.3. Clay mineralogy

Separation of the $< 2 \mu m$ fraction and preparation of the samples for X-ray diffraction (XRD) were performed following the international recommendations of [Kirsch \(1991\)](#). X-ray diffractograms were recorded using a Philips PW 1800 diffractometer with $CuK\alpha$ radiations (50 kV, 30 mA) at angles ranging from 2° to $64^{\circ} 2\theta$ for bulk-sample diffractograms with untreated clay preparations and 2° – $30^{\circ} 2\theta$ for glycolated clay-fraction samples. Xpowder software ([Martin, 2004](#)) was used to determine background levels, and calculate peak intensities and peak areas. The principal clay mineral groups were recognized by their basal spacing at 17 \AA (smectite), at 10 \AA (illite) and 7 \AA (kaolinite + chlorite). Peak areas have been measured in order to estimate semi-quantitative clay mineral content. Estimated semi-quantitative analysis errors range from 5% to 10%; although semi-quantitative analysis aims to show changes or gradients in mineral abundances rather than absolute values. The integrated areas were multiplied by weighting factors ([Biscaye, 1965](#)) and normalized to 100%. Weighting factors are 4 for illite, 2 for kaolinite + chlorite, and 1 for smectite ([Biscaye, 1965](#)).

3.4. X-Ray Fluorescence

Measurements of a total of 23 major and trace element were obtained with a Pioneer-Bruker X-Ray Fluorescence (XRF) spectrometer S4 at the Instituto Andaluz de Ciencias de la Tierra (CSIC) in

Granada, equipped with a Rh tube (60 kV, 150 mA) using internal standards. The samples were prepared in a Vulcan 4 M fusion machine and the analyses performed using a standard-less spectrum sweep with the Spectraplus software.

3.5. Siliceous microfossils

Siliceous microfossil studies were carried out on samples spaced at 10 or 20 cm intervals. For diatom analyses, samples were prepared according to the standard randomly distributed microfossils method. Qualitative and quantitative analyses were done at 1000 magnification using a Leica DMLB with phase-contrast illumination. Counts were carried out on permanent slides of acid-cleaned material (Permount mounting medium). Schrader and Gersonde (1978) recommendations were followed for the counting of microfossil valves. Depending on the diatom abundance, several traverses across each cover slip were examined. A minimum of 350 valves were counted for each sample, when possible.

The silicoflagellate genus *Dictyochoa* and *Distephanus* were counted in order to establish a warm/cold ratio (W/C R) as a function of their abundance. Bohaty and Harwood (1998) and Whitehead and Bohaty (2003) previously have defined *warm/cold ratio* and *silicoflagellate index* respectively. These ratios reflect the relative abundance of *Dictyochoa* and allowed the reconstruction of SSTs and thus the identification of warmer Pliocene periods in the Southern Ocean. In this paper we have defined a modified W/C R by using silicoflagellates total abundance in the following normalized formula: *Dictyochoa* (skeletons/g of dry sediment)/[*Dictyochoa* + *Distephanus* (skeletons/g of dry sediment)]. Values oscillate between 0 and 1 with the highest values indicating warmer temperatures whereas values close to 0 indicate colder temperatures.

3.6. Biogenic opal

Biogenic opal was measured on samples from the same depths as the diatom samples. Samples were dried and ground in an agate mortar. Opal was determined with a sequential leaching technique proposed by De Master (1981) and modified by Müller and Schneider (1993).

3.7. Age model

The age model for the studied sediment core sections was established on the basis of the magnetostratigraphic datums constrain by marine diatom and radiolarian biostratigraphic control, in sediments recovered by Legs 178 and 188 (Barker et al., 1999; O'Brien et al., 2001; Warnke et al., 2004). The age of the paleomagnetic reversals used for both expeditions was based on different time scales: The time scale of Berggren et al. (1995) was used for Sites 1095 and 1096 during Leg 178 (Iwai et al., 2002) and the time scale of Cande and Kent (1995) was used for Site 1165 during Leg 188 (Warnke et al., 2004). For this work we used for all the age models the astronomical tuned timescale of Lourens et al. (1996) assigning corresponding age to the paleomagnetic reversals (Fig. 3). Using the chronology established by paleomagnetic reversals and the sediment thickness between them, sedimentation rates were calculated for the various early to middle Pliocene core intervals (Fig. 3). At Site 1095 the average sedimentation rate is 4.40 cm/ka. The Pliocene interval at Site 1096 was deposited at an average sedimentation rate of 15.88 cm/ka; changing from 14.16 cm/ka during C2An3n to 17.60 cm/ka during C2Ar. At Site 1165 the average middle Pliocene sedimentation rate is 1.53 cm/ka. During C2An3n the sedimentation rate is 2.12 cm/ka, and during C2Ar it is 0.94 cm/ka. Based on the age model and sedimentation rates, sediment samples were dated by linear interpolation between polarity chron boundaries. The studied interval spans the time period 3.7–3.5 Ma at Site 1095, 3.5–3.6 Ma at Site 1096, and 4–3.5 Ma at Site 1165.

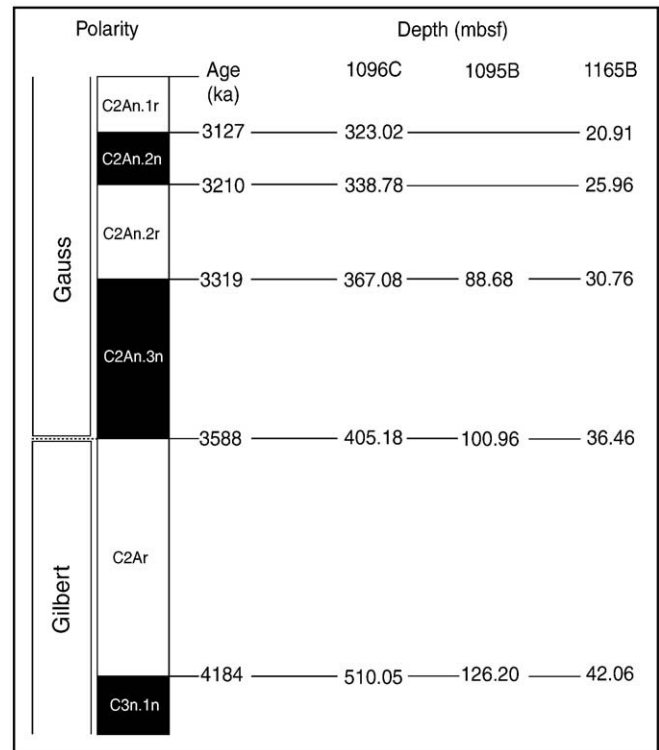


Fig. 3. Age control for the studied sediment sections based on paleomagnetic polarity changes. Corresponding depths below sea floor (mbsf) at each of the studied ODP Sites on the Antarctic Peninsula (Sites 1095 and 1096) and the Prydz Bay (Site 1165) rise are shown. All studied core sections include the Gilbert–Gauss reversal at 3.588 Ma. Age–depth fix points are used to calculate sedimentation rates for these sections, which allow the interpolation of ages within the studied section.

4. Results

Results of the analytical work from this study are presented plotted against depth and ages in Figs. 4–6.

4.1. Sediment facies and textural characteristics

Four main sedimentary facies were identified by lithological descriptions and X-radiographs (Fig. 4):

- Facies 1, laminated mud with silt layers:* finely laminated silty clays with silt layers and silt-rich horizons. Silt layers up to 1 cm-thick have sharp-irregular boundaries and laterally discontinuous thicknesses. Sandy silt horizons (mm-thick) are often laterally discontinuous. The preliminary compositional investigation revealed terrigenous sediments nearly barren of microfossils. This facies was recovered at Site 1095 from 95.52 to 96.20 mbsf and at the base of the studied interval from 103.79 to 105.29 mbsf.
- Facies 2, structureless mud:* structureless fine-grained sediment almost barren of microfossils. This facies was mainly observed at Site 1096.
- Facies 3, mud with silt patches:* fine-grained sediment with silt patches. These sediments are almost barren of microfossils like Facies 2, but contain randomly distributed silt fraction patches. This facies occurs only at Site 1095.
- Facies 4, bioturbated mud:* fine-grained bioturbated sediment with dispersed and/or layered IRD. The preliminary compositional investigation revealed diatom-bearing mud. This facies characterizes Sites 1165, but also occurs at Site 1095, and in the upper part of Site 1096 (Fig. 4). Two thick IRD intervals (up to 10 and 20 cm thick)

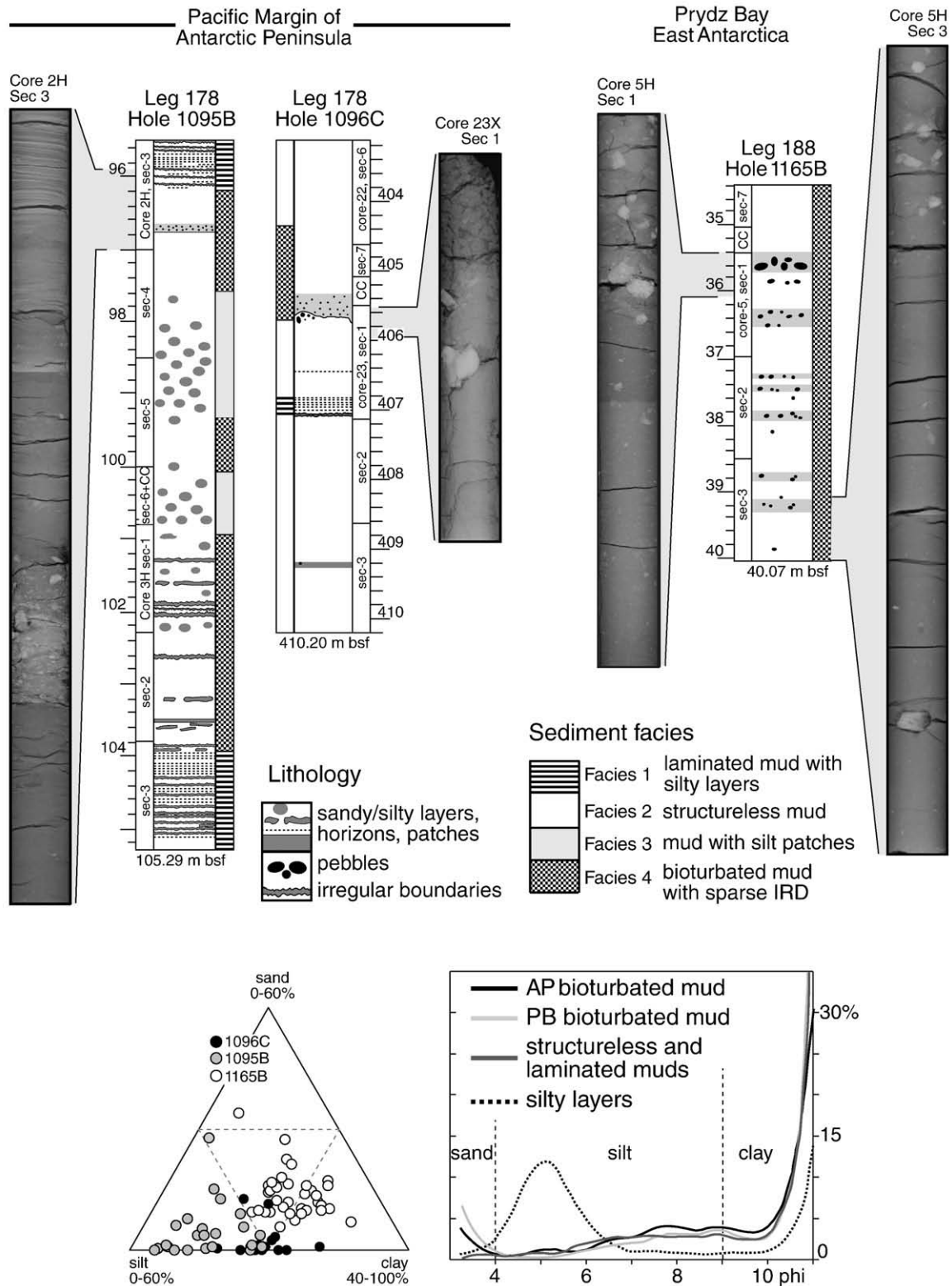


Fig. 4. Core logs and sediment facies of the investigated sequences at ODP Sites 1095, 1096, and 1165. The radiographs relate to three of the four main sedimentary facies: structureless (Facies 2), laminated (Facies 1) and bioturbated muds (Facies 4). The ternary plot shows the sediment texture and the grain-size curves and reveals the grain size distribution within each sedimentary facies. Sediments from Prydz Bay (PB) contain a higher percentage of sands, whereas the sediments from the Antarctic Peninsula (AP) contain a higher percentage of silts. Some silt layers can contain up to 80% of silt (out of the triangle plot).

were found at the top of the sedimentary sequences studied at Sites 1096 and 1165.

The textural analyses of all cores revealed the presence of prevailing fine-grained sediment with the clay fraction often exceeding 50%.

Sediments recovered from the Wild Drift are coarser than those from the Antarctic Peninsula margin, with a higher percentage of sand but a lower content of silt (Fig. 4).

Facies 1 and 2 from Drift 7 contain the finest-grained sediment with less than 1% sand and prevailing fine-grained silt and clay

(clay > 50%, silt \cong 40% average). Facies 4 from the Antarctic Peninsula sites contains 3% (average) sand and a higher percentage of coarse and very-coarse silt than Facies 2 with an average silt content of 47% and a clay content below the 50%.

Facies 4 from Prydz Bay contains a high percentage of sand (9% average), a low content of silt (30% average) with fine-grained silt prevailing, and a high percentage of clay (over 50%).

The grain size distribution within the silt layers of Facies 1 at Site 1095 clearly differ from the other sediment types because of the high silt content (up to 80%). The IRD layers of Facies 4 in Drift 7 contain gravel and occasionally cm-thick pebbles within a sandy-clay matrix with a low percentage of silt (30% average). They have a grain-size spectra very similar to those of the IRD layers in Facies 4 from Prydz Bay.

4.2. Clay mineral assemblages and provenance

The clay mineral assemblage from the Antarctic Peninsula region (Fig. 5) is dominated by illite (40–58% at Site 1095 and 28–45% at Site 1096) and chlorite–kaolinite (33–55% at Site 1095 and 50–70% at Site 1096). Smectite contents vary from 5 to 10% and from 3 to 7% in the samples from Sites 1095 and 1096, respectively. At Site 1095 chlorite–kaolinite concentrations generally increase from 102 mbsf up-section.

The clay mineral assemblage in the samples from Prydz Bay is dominated by illite (50–70%) with lower contents of chlorite–kaolinite (25–38%), and smectite (5–12%). Possible source rocks in the hinterland of Prydz Bay belong to the Pagodroma Group, which comprises the: 1) middle Miocene Fisher Bench Formation and older Mount Johnston Formation that contain a dominance of illite and chlorite assemblages (Ehrmann et al., 2003); 2) the middle-late Miocene Battye Glacier Formation that have a dominance of smectite and kaolinite, and 3) the Pliocene–Pleistocene Bardin Bluffs Formation, which has the highest kaolinite content in absence of smectite.

4.3. Geochemistry

Down core contents of Aluminum (Al), Iron (Fe), Titanium (Ti), and Barium (Ba) are shown in Figs. 5 and 6 as indicative of terrigenous input (Al, Fe, Ti) or biogenic component abundance (Ba/Al ratio). Fe and Ba are presented normalized with the Aluminium that is a relatively stable element (not affected by alteration).

Sediment samples from both West and East Antarctic locations have high Fe and Al contents (Figs. 5 and 6). In samples from Site 1095, Fe values range from 5 to 8% and Al values from 6 to 8%. At Site 1095 Fe and Al contents start to increase at 102 mbsf and 101.2 mbsf and up-section, respectively. Site 1096 samples exhibit Fe and Al values that range from 4 to 5% and 7 to 7.7%, respectively. At Site 1096 a marked decreasing trend up-section of Fe and Al values is seen starting at 405 mbsf. In samples from Site 1165, Fe values range from 3 to 4.7% and Al values range from 5 to 6.5%. At Site 1165, the increasing trend up-section in Fe and Al values starts at 37.7 mbsf (Fig. 6).

Titanium is a trace element indicating terrigenous input, and its content is positively correlated with that of Aluminium at all three sites (Figs. 5 and 6). The Al and Ti contents usually are coherent with the Fe content except for the upper part of Site 1095 above 101 mbsf.

Barium is found in trace amounts at all studied sites. The concentrations of Ba are generally lower in the samples from the Antarctic Peninsula rise with values that vary from 0.05 to 0.15% (Fig. 5). In samples from the East Antarctic margin, the values are higher and range from 0.1 to 0.5% (Fig. 6). The Ba/Al ratio is used as an indicator for biogenic Ba, which is a proxy for biological productivity (cf. Pudsey, 2000; Hillenbrand and Fütterer, 2002). High-percentage of Ba correlates

with the normalized Ba/Al record, and with the biogenic components abundance.

4.4. Siliceous microfossils

Siliceous microfossil assemblages consist of marine diatoms and silicoflagellates. The diatom assemblage analyzed in this study comprises more than 38 taxa with *Fragilariopsis barronii* being the most abundant species (up to 54% of the diatom assemblage) (Figs. 5 and 6). Other significant taxa are *Fragilariopsis interfrigidaria*, *Rouxia antarctica*, *Thalassiosira inura*, *T. torokina*, *T. oestrupii*, *T. tumida*, *Eucampia antarctica* and *Stellarima microtrias*. Silicoflagellate assemblages consist of two genera, *Distephanus* and *Dictyocha*.

Total diatom valve abundance conducted in samples from Site 1095 ranges from 4.3×10^5 to 8.2×10^6 valves/g (average value is 1.97×10^6 valves/g) (Fig. 5). Diatom abundance curves show two main pronounced maxima: from 102 to 101 mbsf with up to 6.02×10^6 valves/g, and from 97.2 to 96.0 mbsf with up to 8.16×10^6 valves/g. A secondary maxima with values around 1.63×10^6 valves/g is observed at 99.7 mbsf. The most abundant taxon, *F. barronii* represents up to 54% of the diatom assemblage. This species shows three maxima roughly corresponding with peaks in total diatom abundance: i) from 104.82 to 101.4 mbsf *F. barronii* exhibits average values of 30% of the assemblage, ii) from 100.02 to 99.40 mbsf the species has values of 25% of the diatom assemblage, and iii) from 97.52 to 96.14 mbsf, the group shows its highest values, with an average of 54% (Fig. 5).

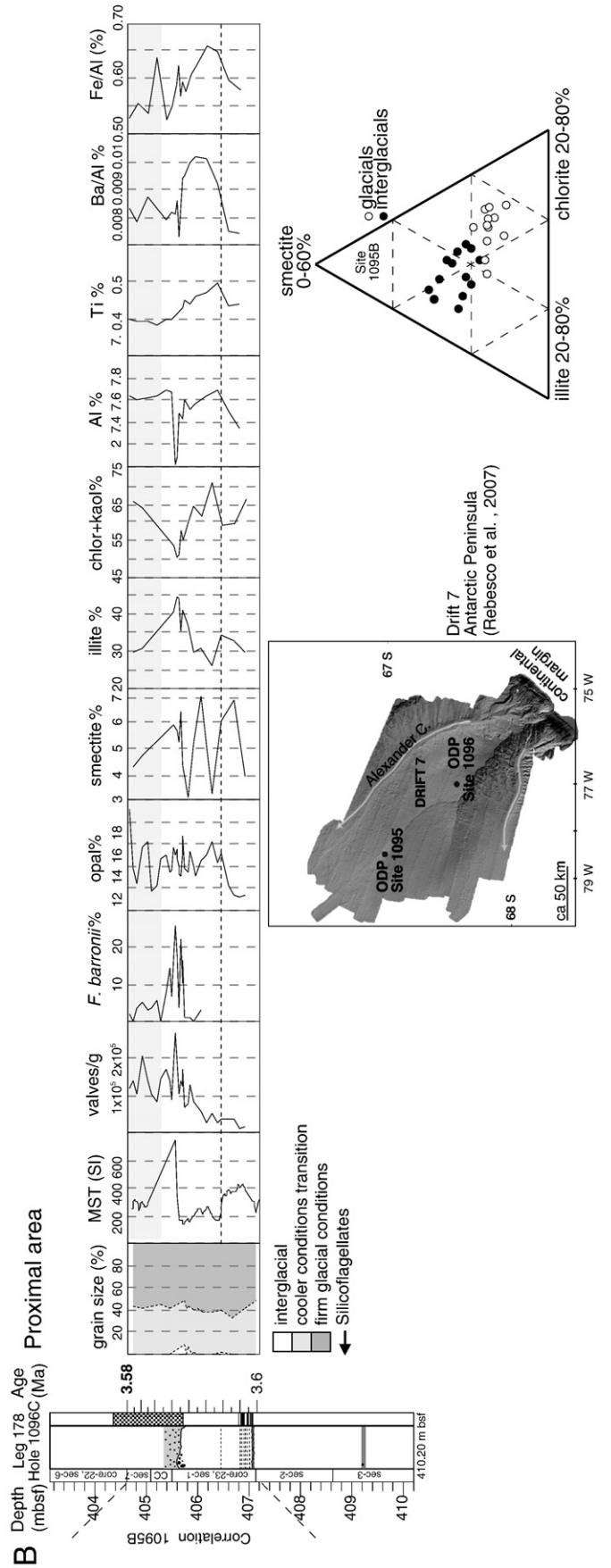
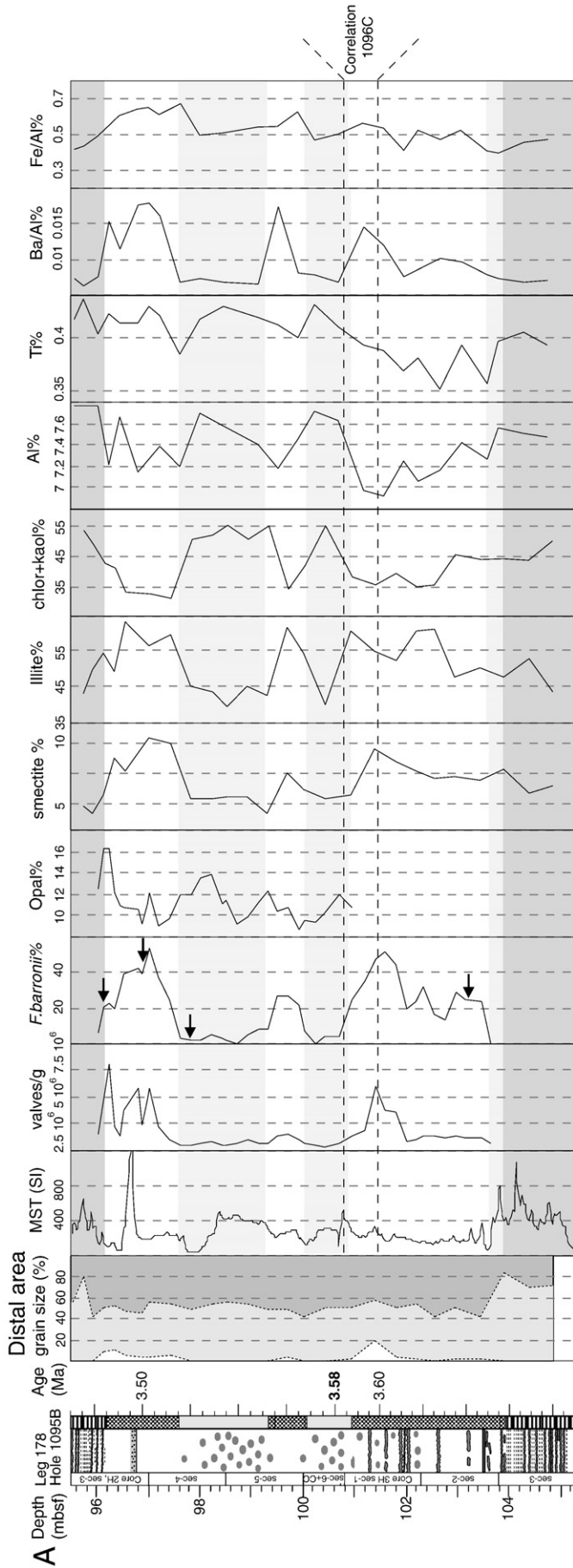
Total abundance of silicoflagellates at Site 1095 is low, only 1.4×10^5 skeletons/g is the highest concentration. The silicoflagellate assemblage is best represented in the upper part of the core from 97.10 to 96.02 mbsf. When present, *Distephanus* is the dominant taxon, and accounts for more than 80% of the abundance. Nevertheless, some specimens of *Dictyocha* have been observed at different depth intervals (96.14, 96.88, 97.83 and 103.20 mbsf) and the W/C R may indicate episodes of warmer sea-surface temperatures (Fig. 5).

Siliceous microfossil analyses conducted in Site 1096 materials show a scarce and poorly preserved diatom assemblage. Diatom abundance is one order of magnitude lower than at Site 1095. The analyzed section can be divided into: i) a lower part, from the base to 405.9 mbsf, with a low diatom abundance (3.78×10^4 valves/g) and, ii) an upper part, from 405.9 to 404.64 mbsf with 1.33×10^5 valves/g and a maximum of 2.5×10^6 valves/g at 405.56 mbsf (Fig. 5). *F. barronii* has an average value of 9.3×10^3 valves/g and makes up an average of 7% of the assemblage. In the section from 405.7 to 405.32 mbsf, however, *F. barronii* averages 14% of the diatom assemblage and has a maximum of 26% at 405.56 mbsf. No silicoflagellates were observed at Site 1096.

Total diatom valve abundance in samples from Site 1165 ranges from 1.38×10^6 to 1.25×10^7 valves/g (average 5.83×10^6 valves/g), which is one order of magnitude higher than at Site 1095. *F. barronii*, the most abundant species, makes up 5.6×10^4 to 4.6×10^6 valves/g (average value of 1.3×10^6 valves/g) (Fig. 6). This taxon follows the same pattern as the total diatom abundance: lower values below 7.46×10^5 valves/g and *F. barronii* contents of 6.1% are recorded from the base to 38.05 mbsf. From 38.05 mbsf to the section top, absolute diatom and *F. barronii* abundance increases from <10% to 15–40%. This interval is characterized by well-defined abundance fluctuations with amplitudes accounting for concentration changes of about 10%. A marked minimum in *F. barronii* abundance down to 6% can be observed between 36.9 and 36.5 mbsf, and a secondary minimum can be observed between 35.59 and 35.15 mbsf (Fig. 6).

Total abundance of silicoflagellates at Site 1165 is higher than for Site 1095 with an average content of 1.35×10^5 skeletons/g and a

Fig. 5. Sedimentological, magnetic susceptibility (MST), siliceous microfossil abundances, biogenic opal, and mineralogical and geochemical parameters plotted vs. depth and age for (A) Site 1095 and (B) Site 1096. Note that Site 1096 contains an expanded record between 3.58 and 3.59 Ma, which is correlated with Site 1095. The ternary plot shows the differences in the clay mineralogy record from Site 1095 between interglacial periods (enhanced smectite) and glacial periods (enhanced chlorite) (Rebesco et al., 2007).



maximum up to 4.4 skeletons/g. Silicoflagellates are present throughout the studied section, but from 35.64 mbsf they become more abundant towards the top (Fig. 6). *Distephanus* is the dominant taxon, and makes up more than 88% of the abundance. W/C R and *Dictyocha* relative abundance follow the same pattern. *Dictyocha* has an average content of 9% and it is significantly more abundant at three intervals, coinciding with the established W/C R: 37.62 to 37.30 mbsf (average abundance of 59.40% with maximum values up to 85%, W/C R up to 0.75); 35.92 to 35.64 mbsf (average abundance of 16%, W/C R up to 0.25) and 35.17 to 34.95 mbsf (average abundance of 8.3%, W/C R up to 0.10). Several smaller maxima can be observed at the lower part of the section (Fig. 6). The *Dictyocha* interval between 37.62 and 37.30 mbsf includes the 60% values at 37.60 mbsf previously reported by Whitehead and Bohaty (2003) from Site 1165 and interpreted to indicate a SSST of about 5.6 °C above present level.

4.5. Biogenic opal

The biogenic opal content west of the Antarctic Peninsula varies between 9 to 15 wt.% in samples from Site 1095, and 11 to 19 wt.% in samples from Site 1096 (Fig. 5). In samples from Prydz Bay (Site 1165) the biogenic opal content varies from 15 to 30 wt.% (Fig. 6).

The interval between 38.5 and 36 mbsf at Site 1165, exhibits enhanced biogenic opal concentrations (up to 20–27%). Similar to the *F. barronii* record, the opal concentration in this interval is characterized by pronounced variations with amplitudes of about 10%.

5. Discussion

5.1. Climate proxies

In areas dominated by hemipelagic sedimentation, biogenic abundance may be controlled by both the variance in terrigenous supply and biogenic production. The down-core coeval increase in the Ba record, the *F. barronii* and total diatom abundance, and the biogenic opal (Figs. 5 and 6), suggests that biogenic processes are controlling the changes. According to Zielinski and Gersonde (2002) and Cortese and Gersonde (2008), *F. barronii* is assumed to be the evolutive precursor of *F. kerguelensis*, and speculate that both species lived under similar SSST conditions. In this sense, *F. kerguelensis* shows a dwelling preference of open-ocean conditions with summers free of sea-ice and SSST between 1 and 12 °C (Crosta et al., 2005) corresponding to the modern Antarctic Zone and the Polar Frontal Zone. Pleistocene SSST reconstruction based on diatom transfer function indicates a relationship between increased *F. kerguelensis* abundance and SST during interglacials (Zielinski and Gersonde, 1998). Moreover, Cortese and Gersonde (2008) affirm that *F. barronii* during the warm middle Pliocene, as well as *F. kerguelensis* during the middle-late Pleistocene, are the main carriers of organic matter and nutrients to the deep-ocean, these species were/are the main contributors to the production of the biogenic opal and export productivity to the Southern Ocean.

Based on the close positive correspondence between the peaks in silicoflagellate W/C R at Sites 1095 and 1165 and the indicators for higher biogenic productivity (Figs. 5 and 6) we interpret these events to record high biogenic productivity during interglacial warm climate conditions. The observed enhancement of smectite corresponding with interglacial periods in sediments from Site 1095 (Fig. 5) had been interpreted in previous studies to result from bottom-current transport of smectite along the continental rise, from its source on the continental shelf northwest of the Antarctic Peninsula, during interglacial climate periods (Hillenbrand and Ehrmann, 2001; Lucchi et al., 2002; Hillenbrand and Ehrmann, 2005; Hepp et al., 2006).

Down-core changes in the distribution of the two detrital elements Al and Ti indicate variability in the terrigenous supply to our sites. Higher supply of terrigenous detritus between the warm intervals,

could be caused by advances of glaciers/ice-sheets during cold glacial conditions across the shelf or through proglacial meltwater plumes and sediment gravity flows during the deglaciation period. The laminated sedimentary facies that characterize the intervals of higher terrigenous supply at Site 1095 and the enrichment in chlorite in Drift 7 sediments, previously have been interpreted to occur under glacial conditions (e.g., Pudsey, 2000; Hillenbrand and Ehrmann, 2001; Lucchi et al., 2002; Hepp et al., 2006).

5.2. Early Pliocene interglacial record: biogenic productivity and sedimentary processes

5.2.1. Antarctic Peninsula

Sediments from Site 1095 record three main intervals of enhanced biogenic productivity during interglacial climates that are identified by a positive correlation between peaks in *F. barronii* abundance, presence of silicoflagellates and maxima of biogenic opal and biogenic Ba content. These intervals are located between 104.8–101.4, 100–99.4, and 97.8–96 mbsf (Fig. 5). Peaks of productivity correlate positively with enhanced illite and smectite contents, and correlate inversely with values of Al, Ti, Fe, MST, and chlorite–kaolinite (Fig. 5). Based on our age model, these depth intervals of enhanced biogenic productivity occur between 3.7–3.6 Ma and 3.5 Ma, respectively. Within these time intervals, the highest productivity peaks are recorded at 103.5, 102.5, 101.6, and 99.7 mbsf (3.6 Ma), and 98.2, 97, 96.2 and 94.1 mbsf (3.5 Ma) (Fig. 5). Siliceous microfossil assemblages suggest that during these interglacial periods there was low or no sea-ice above Site 1095 because sea-ice related taxa were not recorded in the diatom assemblage. At Site 1096, interglacial conditions are indicated between 406 and 405 mbsf by peaks in *F. barronii* and biogenic Ba coinciding with the magnetic polarity reversal (Gilbert-Gauss) at 3.58 Ma (Fig. 5).

Interglacial sediment facies at Sites 1095 and 1096 consist of bioturbated diatom-bearing sandy mud with both sparse and layered IRD (Facies 4). Thick IRD layers and/or coarser grained sediments correspond to maximum peaks of bio-productivity (Figs. 4 and 5). In sediments deposited by the Laurentian Ice Sheet, well-dated major instabilities of the ice sheet are manifested as beds of ice rafted detritus that is deposited during deglaciation (Skene and Piper, 2003). The marine sediment facies located off the Antarctic Peninsula, with both sparse and layered ice-rafted detritus, suggest a significant increase of the APIS calving during the interglacial intervals with open water conditions and no sea-ice cover above these offshore sites.

The marine clay mineral assemblage off the Antarctic Peninsula during interglacial intervals is dominated by illite (>40%) with higher values of smectite and minor values of chlorite–kaolinite with respect to glacial intervals (Fig. 5). According to Lucchi et al. (2002) and Hillenbrand et al. (2008), the illite in this area is delivered through sub-glacial meltwater plumes, whereas smectite-rich sediments are transported by bottom contour currents coming from the South Shetland Islands (the “smectite province” of Hillenbrand and Ehrmann, 2001 located north of 64°S). The lack of lamination associated to contour currents is explained by high bioturbation of sediments and/or low flow strength. The higher values of both illite and smectite during interglacials is related to a minor input of chlorite–kaolinite rather than a higher strength or efficiency of both contour currents and turbid meltwater plumes. The chlorite derives from the ablation of the crystalline basement and it is delivered into the area by down-slope mass transport largely occurring during glacials when the grounded-ice reached the shelf edge (Hepp et al., 2006).

At Site 1095, three warm episodes were detected based on sediment facies (i.e., 102.8–101 mbsf, 100–99.4 mbsf, and 97.6–96.2 mbsf) (Fig. 4); these episodes coincide closely with the high-productivity and coarser grained intervals. At Site 1096 only one minor warm episode was detected (407.2–405.6–404.4 mbsf), in which coarser-grained

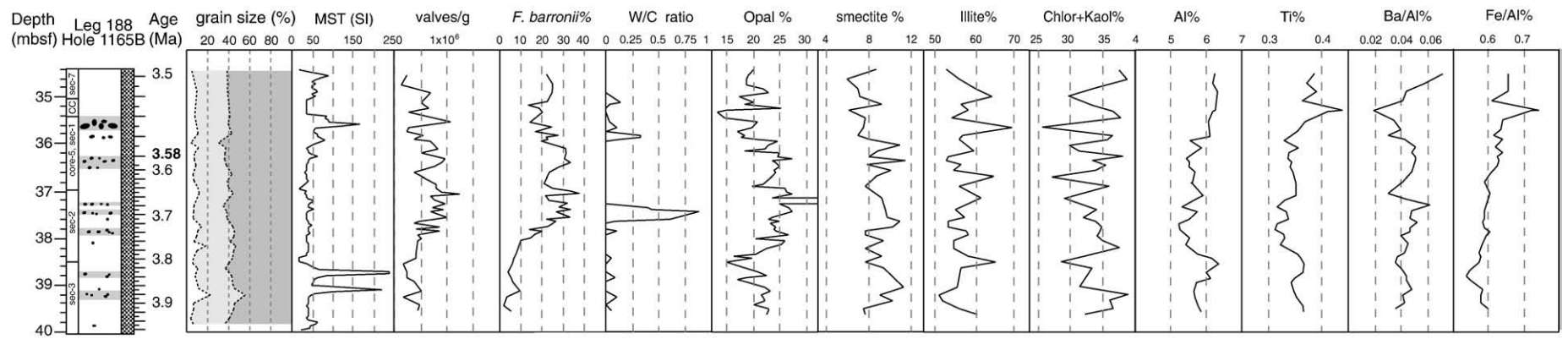


Fig. 6. Sedimentological, magnetic susceptibility (MST), siliceous microfossil abundances, biogenic opal, and mineralogical and geochemical parameters plotted vs. depth and age for Site 11655.

sediments are characterized by moderate productivity and are confined by almost barren glacial sediments nearly barren of microfossils.

5.2.2. Prydz Bay

Prydz Bay Site 1165 records two main intervals of enhanced biogenic productivity that are marked by increased abundance of *F. barronii*, which roughly coincide with increased biogenic Ba content between 37.8–36.8 mbsf and 36.6–34.8 mbsf (Fig. 6). Based in our age model these two higher biogenic productivity intervals took place between 3.7 and 3.5 Ma, respectively. Diatom assemblages indicate that open water marine conditions with no sea-ice characterize these intervals of warmth. This is in agreement with previously published data by Whitehead et al. (2005) who applied the *Eucampia antarctica* Index and observed that during our studied interval the area experienced a significant reduction of winter sea-ice concentration (60% less than today). Individual peaks of high biogenic productivity are recorded at 39.15 mbsf (3.9 Ma), 37.7, 37.35 and 37 mbsf (3.7 Ma), 36.3 and 36 mbsf (3.6 Ma), and 35.23 and 34.5 mbsf (3.5 Ma). The peaks at 36 mbsf coincide with the magnetic polarity reversal (Gilbert–Gauss) at 3.58 Ma.

The silicoflagellate W/C R record from Site 1165 shows three main intervals of warmth within the studied section. Based in our age model, the lower warm interval occurs at 3.7 Ma (37.62 and 37.34 mbsf). This interval includes the 60% *Dictyocha* values at 37.60 mbsf reported by Whitehead and Bohaty (2003) from Site 1165 and interpreted to indicate a mean annual SSST of about 5.6 °C above modern level. Our data reveals W/C R up to 0.75 (*Dictyocha* average abundance values of 59.4%, up to 85%) within this interval, which indicate SSSTs even higher than those postulated by the former authors. A younger interval in W/C R is recorded at 3.6–3.5 Ma (36 and 35.54 mbsf), with the maximum occurring at about 3.6 Ma (35.8 mbsf). The W/C R (0.25) and the *Dictyocha* percentage values (16.4%) in this interval would be tentatively indicative of SSSTs between 2.7° and 4 °C above present levels. The silicoflagellate record at 3.5 Ma (35.1 mbsf) (W/C R up to 0.10 and *Dictyocha* average abundance of 8.3%), would suggest SSSTs of 2.5 °C above modern level.

The radiograph facies and grain size distribution in the sediments recovered from Site 1165 are remarkably uniform throughout the studied interval (Fig. 4). The bioturbated mud, Facies 4, is the only facies observed and contains a relatively high percentage of sand (9%) with a lower silt content with respect to the sites studied in the Antarctic Peninsula. Ice rafted debris pebbles are randomly sparse throughout the studied interval (both glacial and interglacial). Previous sedimentological studies on Site 1165 indicated a major textural change at 3.5 Ma with younger finer grained sediments sited above the studied interval (Passchier, 2007).

The biostratigraphic investigation allowed the identification of intervals of warm climatic conditions that cannot be univocally supported by evidence in the sediment facies, structures or composition (XRD or XRF) except for a higher concentration of IRD consisting on gravel and cm-thick pebbles (see correlation between the IRD distribution on the core log and the W/C R, Fig. 6).

5.3. Early Pliocene glacial record: terrigenous supply and sedimentary processes

5.3.1. Antarctic Peninsula

At Site 1095, intervals of increased terrigenous sediment supply are indicated by a positive correlation between peaks of Al, Ti, chlorite–kaolinite at 104.4–103.8 mbsf (3.7 Ma), 103, 100.6–100.1 mbsf (3.6 Ma), and 99.4–97.8 mbsf (3.5 Ma) (Fig. 5). Our record shows that after 3.6 Ma Al, Ti, and chlorite–kaolinite concentrations increased (Fig. 5). We interpret this increase as the start of an overall cooling trend beginning at 3.6 Ma. Terrigenous supply to Site 1095

(Fig. 5) is characterized by peaks in chlorite–kaolinite (406.2 mbsf), Ti and Al at 406.4 mbsf and 405.2 mbsf.

Glacial sedimentation is characterized by laminated and structureless mud, and sediments with silt-patches (Facies 1, 2, 3). All sediment facies are characterized by a clay mineral assemblage dominated by chlorite–kaolinite with lower percentages of illite (25–30%) and smectite (10–15%) with respect to interglacials, indicating a predominance of down-slope gravity input of sediments (Fig. 5).

The laminated sediments (Facies 1) contain more coarse-grained silt, whereas the structureless mud (Facies 2) and the silty-patched mud (Facies 3) are dominated by fine-grained and medium-grained silt respectively. The lack of biogenic components in Facies 1, 2, and 3 indicate reduced productivity from unfavourable environmental conditions and/or dissolution of biogenic particles (e.g. presence of few and fragmented diatoms badly preserved). The absence of clearly evident bioturbation in Facies 2 and the presence of undisturbed laterally continuous laminations in Facies 1 confirm reduced benthos activity with lamination produced by either contour currents or gravity driven flows generating shear stress at the sea bottom.

Structureless and laminated muds were previously described on the late Quaternary sedimentary sequence and were interpreted to represent glacial and/or transitional climatic conditions (Pudsey and Camerlenghi, 1998; Pudsey, 2000; Lucchi et al., 2002; Lucchi and Rebecco, 2007). Accordingly, we ascribe Facies 1 to full glacial conditions and Facies 2 to less severe cold conditions (Site 1096), in which the lack of lamination indicates little or no shear stress at the sea-bottom (either weak bottom currents or little influence by gravity flows due to the more elevated site over the channel system).

Mud with silty patches (Facies 3) observed in sediments from Site 1095 alternates with the bioturbated mud (Facies 4, interglacial facies). We suggest that Facies 3 was also deposited during minor cold climatic conditions under the influence of both gravity and contour currents. A similar sediment facies was described for silty/muddy contourites in which silt patches (mottles) are produced by bioturbation of the silt fraction (Stow et al., 2002; Stow and Faugères, 2008). We suggest a combination of contour currents generating the silt patches and turbidity currents that delivered sediments with a high chlorite content. The absence of Facies 3 at Site 1096 may be related to a minor influence of bottom-contour and turbidity currents on the sedimentation at this site, because of its more elevated location on Drift 7 (Fig. 1). Lucchi et al. (2002) reported reduced clay mineral values of both contour current-driven smectite during interglacials and turbidity flow-driven chlorite during glacial at the summit of Drift 7.

5.3.2. Prydz Bay

Enhanced terrigenous sediment supply to Site 1165 is indicated by higher Al, Ti, and illite contents and low values of biogenic Ba and *F. barronii* at 38.45 mbsf (3.8 Ma), 37 and 35.8 mbsf (3.6 Ma), and 35.3 and 34.85 mbsf (3.5 Ma). An increase of Ti, Fe, Al and K concentrations similar to that observed at Site 1095 starts at 3.7 Ma. The biostratigraphic and geochemical investigation allows the identification of intervals of colder climatic conditions. The glacial intervals are not univocally supported by sediment structures or composition, because sediment facies and grain size distribution is remarkably uniform throughout the studied interval (Fig. 4). The sandy bioturbated mud with randomly sparse IRD (Facies 4) at Site 1165, may indicate more stable current conditions, in which sediment delivery to the slope and rise mainly resulted from IRD supply.

5.4. The circum-Antarctic record of warm and cold Pliocene events

We correlated the ages assigned to the sections of Sites 1095, 1096 and 1165 with the Marine Isotopic Stages of standard oxygen isotope curve proposed by Lisiecki and Raymo (2005) (Fig. 7). Correlations

show interpreted warm events in the Antarctic sites coinciding with interglacial stages in the isotopic records (Fig. 7). Using our age model, periods of warmth are recorded in both the Antarctic Peninsula and Prydz Bay regions, which correlate with isotopic stages Gi5, Gi1, MG11, and MG7 (Fig. 7). This finding suggests a coeval response to warming of both the APIS and the EAIS. The circum-Antarctic event corresponding to isotopic stage MG11 coincides with the section dated by the magnetic polarity reversal (Gilbert-Gauss) at 3.58 Ma (Fig. 3). MG11 also coincides with the interval when the silicoflagellate warm/cold index at Site 1165 indicates tentative SSSTs 2.7°–4 °C above present level. Based in our age model and calculated sedimentation rates glacial–interglacial cyclicity between 3.7 and 3.5 Ma in the cores from Antarctic Peninsula and Prydz Bay Sites, result in average frequencies between 40 and 10 kyr consistent with obliquity and precession forcing.

We observe that isotopic stage Gi5 is one of the warmest and longest lasting interglacials within the studied time interval. During this interglacial SSST data from Site 1165 indicates open water conditions in the absence of sea-ice. SSST during this interval, as suggested by the silicoflagellate warm/cold ratio was >5.6 °C above present. Similarly, isotopic stages MG11 and MG7 occur during a prolonged period of warmth characterized by low-amplitudes in glacial–interglacial cyclicity (Fig. 7). Our records indicate that these intervals were characterized by warmer surface waters and less sea-ice. This is supported by 1) our interpretation of the abundance of *F. barronii* and the lack of sea-ice related taxa; 2) enhanced biogenic opal concentrations (average 14 wt.% in the Antarctic Peninsula and 27.5 wt.% in Prydz Bay) compared to late Quaternary concentrations (average 8 wt.%) (cf. Hillenbrand and Fütterer, 2002; Hepp et al., 2006); and 3) the silicoflagellate W/C R from Site 1165 (Fig. 6). In addition, the retreat of ice sheets during this interval of prolonged warmth is suggested by the bioturbated and IRD-enriched facies that characterize these high-productivity intervals. For previous warm periods, other studies suggest that the warm conditions result from strengthened Northern Component Water (NCW) influx into the Southern Ocean and increased heat input and upwelling of CDW close to the shelf break. This causes warmer surface water conditions south of the APF (e.g., Hillenbrand and Fütterer, 2002; Grützner et al., 2005; Hepp et al., 2006).

An increase of the terrigenous sediment supply at all our sites starting between 3.7 and 3.6 Ma suggest that this prolonged warm period was superimposed on a cooling trend. A cooling trend is also supported by the onset of global sea level drop at 3.6 Ma (Haq et al., 1987; Krantz, 1991) (Fig. 7). We postulate that, although the start of a cooling trend is recorded at about 3.7–3.6-Ma at our sites, relatively warm conditions prevailed until 3.6–3.5 Ma and maintained open marine conditions with reduced or no sea-ice and reduced ice sheet volume and extent. The start of the cooling trend coincided with a decrease in SSST as indicated by the silicoflagellate W/C R from Site 1165, which indicates an overall decrease from 5.7 °C at 3.7 Ma to 4°–2.7 °C at 3.6 Ma, and 2.5 °C at 3.5 Ma.

Coeval glacial events based on our age model are recorded at the Antarctic Peninsula and in Prydz Bay between the warm intervals. In contrast to the late Quaternary sequence, in the late Pliocene drift sediments from the Antarctic Peninsula rise, the transition from interglacial to glacial conditions appears to be abrupt with IRD-rich sediments truncated by the onset of laminated sediments (Fig. 4). Hepp et al. (2006) describe the same type of transition for older early Pliocene sediments. Although we see evidence in our records for ice sheet reduction, we agree with the conclusion of Hepp et al. (2006) and Smellie et al. (2009) that the APIS did not fully collapse during the interglacial intervals, which allowed a rapid onset of the glacial down-slope gravity transport processes during colder conditions. This conclusion is consistent with the interglacial clay mineral assemblage that is dominated by illite (>30%) delivered to the continental slope and rise through sub-glacial meltwater plumes at the glacial terminus

(see Section 5.2.1). A fully retreated ice-sheet would have prevented the water plumes to reach the slope and rise and the sediments would have been trapped on the shelf (similar to today).

A highly dynamic glacial regime during the early Pliocene is shown by pronounced variability in the down-core distribution of sediment parameters and sedimentary facies, which is better recorded on the Antarctic Peninsula margin than in Prydz Bay. This variability may result from differences in sediment delivery by the ice sheets on the two margins. The Antarctic Peninsula sites may record a more dynamic behavior of the APIS (i.e., faster response of the ice sheet to cooling and warming). We attribute the uniform down-core pattern of proxies and facies at Site 1165 to a slower response of the terrestrial EAIS to climate change.

6. Conclusions

Our study shows that the application of uniform methodologies to the high-resolution study of multiple proxies from the same core intervals can yield a record of changes in primary biogenic productivity (siliceous microfossils, biogenic opal, biogenic Ba), terrigenous supply (e.g., Al, Ti), and sedimentary processes (sedimentary facies, textures and clay mineralogy) that can be combined to interpret a robust history of glacial–interglacial cyclicity.

Four circum-Antarctic warm events/intervals are recorded in the studied Pliocene section. Warm conditions in both East and West Antarctica are recorded, which based in our age model correspond to isotopic stages Gi5, Gi1, MG11 and MG7. Our records indicate these are periods of prolonged or extreme warmth. For the Gi5 interglacial our data corroborates the 60% *Dictyochoa* percentage at 34.60 mbsf reported by Whitehead and Bohaty (2003) interpreted to indicate a SSST of about 5.6 °C above present. Our higher-resolution sampling interval shows *Dictyochoa* percentages up to 87.5%, which indicates SSST >5.6 °C above present levels. During MG11, which coincides with the section dated by the magnetic polarity reversal Gilbert-Gauss at 3.58 Ma, SSSTs were 2.5°–4° warmer than present and reduced sea-ice cover in Prydz Bay and probably also west of the Antarctic Peninsula, is indicated by increased primary productivity. In addition, a reduction of ice sheet size is suggested by the bioturbated and IRD-enriched facies that characterizes these high-productivity intervals. Based in our age model and calculated sedimentation rates glacial–interglacial cyclicity between 3.7 and 3.5 Ma in the cores from Antarctic Peninsula and Prydz Bay Sites, result in average frequencies at the obliquity and precession forcing.

An increase of the terrigenous sediment supply at all our sites starting between 3.7–3.6 Ma suggest that this prolonged warm period was superimposed on a cooling trend also recorded by the decrease in SSSTs (from >5.6 °C at 3.7 Ma to 4°–2.7 °C at 3.6 Ma, and 2.5 °C at 3.5 Ma.) indicated by the silicoflagellate W/C R from Site 1165. We postulate that, although the start of a cooling trend is recorded at about 3.7–3.6-Ma at our sites, relatively warm conditions prevailed until 3.6–3.5 Ma and maintained open marine conditions with reduced or no sea-ice and reduced ice sheet volume and extent.

These results from two regions of the Southern Ocean, when combined with new information from the ANDRILL AND-1B drillcore in the western Ross Sea (Naish et al., 2009), provide a continent-wide perspective on Pliocene ice sheet behavior in response to climate changes. These data, when linked to modeling studies like those of Pollard and DeConto (2009) will further our understanding of how these ice sheets may respond to future warming of the southern high latitudes. Future studies from the marine realm, integrated with on-land studies such as those from the Pagodroma and Sirius Group, (Harwood, 1983; Harwood and Webb, 1986, 1991; Webb et al., 1996; Francis and Hill, 1996), will be required to understand the level and the duration of early-middle Pliocene warming and its impact on the EAIS.

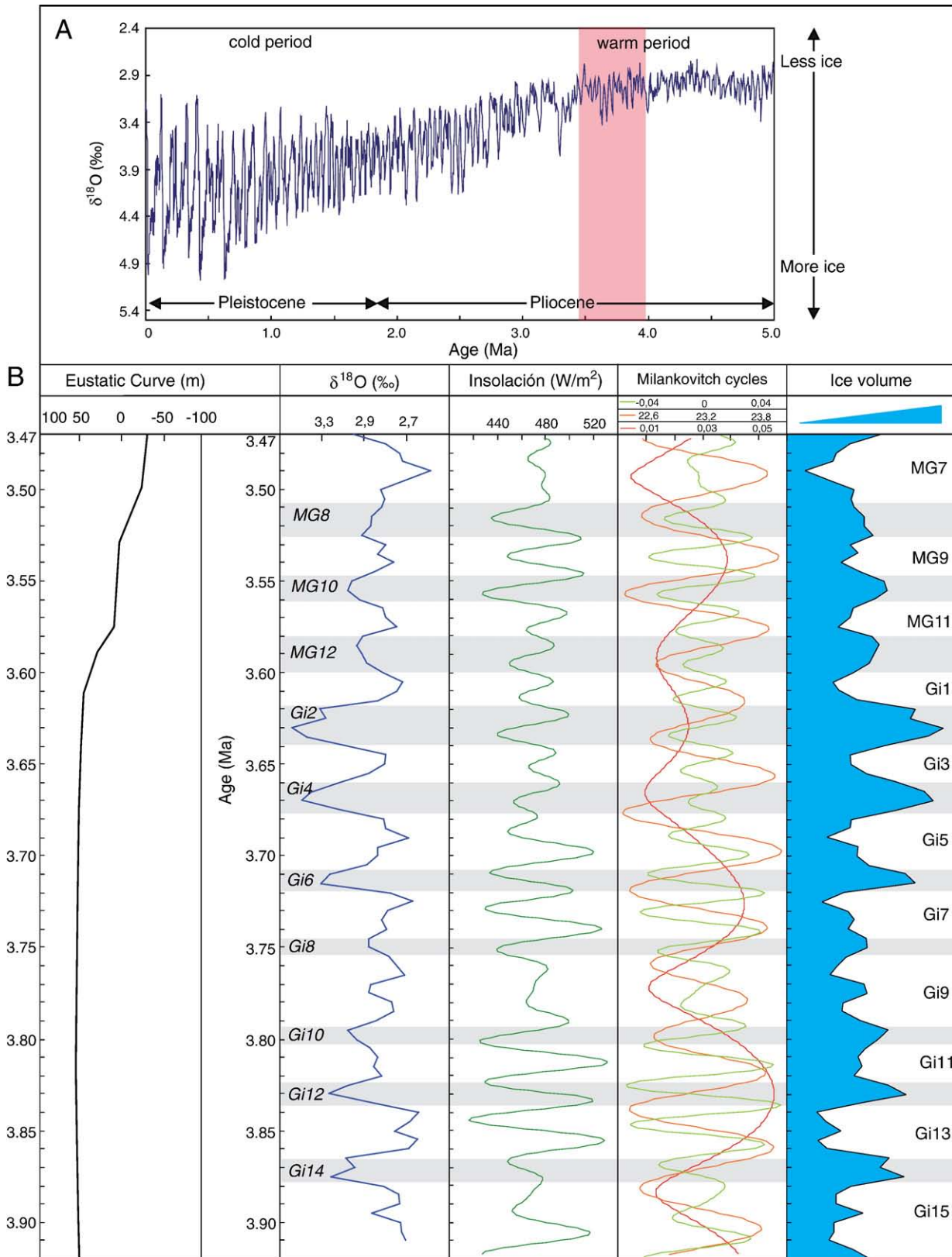


Fig. 7. A) Benthic foraminifera $\delta^{18}\text{O}$ record for the past 5 Ma (Lisiecki and Raymo, 2005). The shadowed interval indicates the studied interval. B) Isotopic model after Lisiecki and Raymo (2005) for the studied age interval. This curve shows the four warm circum-Antarctic events correlated to interglacial isotopic stages based in our age model and the paleoclimate indicators used for this study. Refer to text for details about paleoenvironmental conditions (i.e., sea ice extent, inferred Surface Water temperatures, and ice sheet behavior) during these circum-Antarctic warm intervals. The MG11 stage coincides with the sedimentary section in our cores dated by the magnetic polarity reversal Gilbert -Gauss at 3.58 Ma.

Acknowledgements

The authors want to thank the Integrated Ocean Drilling Program for providing the samples used in this study. We thank Walter Hale and the staff at the IODP Bremen Core Repository for all their help prior to and during the sampling party, and Tobias Moerz and Daniel Hepp for providing the X-Ray images of selected intervals. We thank Hans Nelson for reviewing a preliminary draft of this paper and Claus-Dieter Hillenbrand and Sandra Passchier for their valuable review comments, which greatly improved this manuscript. The research in this paper has been supported by the Spanish Ministry of Science and Education Grants: REN2003-0922-CO2-01 and POL2006-072667/CGL. Additional support received by Grant CSD2007-00067.

References

- Barker, P.F., Camerlenghi, A., Acton, G.D., et al., 1999. Proceedings of the Ocean Drilling Program: Initial Reports, vol. 178 (CD-ROM). Available from: Ocean Drilling Program, Texas A&M University, College Station, TX 77845-9547, U.S.A.
- Barker, P.F., Camerlenghi, A., Acton, G.D., Ramsay, A.T.S. (Eds.), 2002. Proceedings of the Ocean Drilling Program: Scientific Results, vol. 178 (CD-ROM). Available from: Ocean Drilling Program, Texas A&M University, College Station, TX 77845-9547, U.S.A.
- Berggren, W.A., Kent, D.V., Swisher, C.C., Aubry, M.P., 1995. A revised Cenozoic geochronology and chronostratigraphy. In: B.W.A., Kent, D.V., Aubry, M.P., Hardenbol, J. (Eds.), *Geochronology, time scales and global stratigraphic correlation: Spec. Publ.-SEPM (Soc. Sediment. Geol.)*, pp. 129–212.
- Biscaye, P.E., 1965. Mineralogy and sedimentation of recent deep-sea clay in the Atlantic Ocean and adjacent areas and oceans. *Geol. Soc. Am. Bull.* 76, 803–832.
- Bohaty, S.M., Harwood, D.M., 1998. Southern Ocean Pliocene paleotemperature variation from high-resolution silicoflagellate biostratigraphy. *Marine Micropaleontology* 33, 241–272.
- Cande, S.C., Kent, D.V., 1995. Revised calibration of the geomagnetic polarity timescale for the Late Cretaceous and Cenozoic. *Journal of Geophysical Research* 100, 6093–6095.
- Cortese, G., Gersonde, R., 2008. Plio/Pleistocene changes in the main biogenic silica carrier in the Southern Ocean, Atlantic sector. *Marine Geology* 25, 100–110.
- Crosta, X., Pichon, J.J., Romero, O., Armand, L.K., 2005. The biogeography of major diatom taxa in Southern Ocean sediments: 2. Open ocean related species. *Palaeogeography, Palaeoclimatology, Palaeoecology* 223 (1), 66–92.
- De Master, D.J., 1981. The supply and accumulation of silica in the marine environment. *Geochimica Cosmochimica Acta* 45, 1715–1732.
- Dowsett, H., Barron, J., Poore, R.Z., 1996. Middle Pliocene sea surface temperatures: a global reconstruction. *Marine Micropaleontology* 27, 13–25.
- Ehrmann, W., Bloemendal, J., Hambrey, M., McKelvey, B., Whitehead, J., 2003. Variations in the composition of the clay fraction of the Cenozoic Pagodroma Group, East Antarctica: implications for determining provenance. *Sedimentary Geology* 161 (1–2), 131–152.
- Francis, J.E., Hill, R.S., 1996. Fossil plants from the Pliocene Sirius Group, Transantarctic Mountains: evidence for climate from growth rings and fossil leaves. *Palaios* 11, 389–396.
- Freedman, G.M., Sanders, J.E., 1978. *Principles of Sedimentology*. John Wiley and Sons, New York, 792 pp.
- Gordon, A., Molinelli, E., 1982. *Southern Ocean Atlas: thermohaline and chemical distributions*. Columbia University Press, NY.
- Grützner, J., Hillenbrand, C.-D., Rebesco, M., 2005. Terrigenous flux and biogenic silica deposition at the Antarctic continental rise during the late Miocene to early Pliocene: implications for ice sheet stability and sea ice coverage. *Global and Planetary Change* 45, 131–149.
- Hambrey, M.J., Ehrmann, W.U., Larsen, B., 1991. Cenozoic glacial record of the Prydz Bay continental shelf, East Antarctica. In: Barron, J., Larsen, B., et al. (Eds.), *Proceedings of the Ocean Drilling Program. Scientific Results*, vol. 119. Ocean Drilling Program, College Station, TX, pp. 77–132.
- Haq, B.U., Hardenbol, J., Vail, P.R., 1987. Chronology of fluctuating sea levels since the Triassic. *Science* 235, 1156–1167.
- Harwood, D.M., 1983. Diatoms from the Sirius Formation, Transantarctic Mountains. *Antarctic Journal of the United States* 18 (5), 98–100.
- Harwood, D.M., Webb, P.N., 1986. Recycled siliceous microfossils from the Sirius Formation. *Antarctic Journal of the United States* 21 (5), 101–103.
- Harwood, D.M., Webb, P.N., 1991. Early interpretations of Antarctic and Arctic glacial history: uniformitarian biases mask a dynamic history of Cenozoic ice-volume variation. *Geological Society of America Abstracts with Programs* 25 (5), 106.
- Harwood, D.M., McMinn, A., Quilty, P., 2000. Diatom ages of Sorsdal Formation, Vestfold Hills, Antarctica. *Antarctic Science* 14 (4), 443–462.
- Haywood, A.M., Valdes, P.J., Sellwood, B.W., 2000. Global scale palaeoclimate reconstruction of the middle Pliocene climate using the UKMO GCM: initial results. *Global and Planetary Change* 25 (3/4), 239–256.
- Haywood, A.M., Smellie, J.L., Ashworth, A.C., Cantrill, J., Florindo, F., Hambrey, M.J., Hill, D., Hillenbrand, C.D., Hunter, S.J., Larter, R.D., Lear, C.H., Passchier, S., van de Wal, R., 2009. Middle Miocene to Pliocene history of Antarctica and the Southern Ocean. In: Florindo, F., Sievert, M. (Eds.), *Antarctic Climate Evolution: Developments in Earth and Environmental Sciences*, vol. 8, pp. 401–464.
- Hepp, D.A., Moerz, T., Grützner, J., 2006. Pliocene glacial cyclicity in a deep-sea sediment drift (Antarctic Peninsula Pacific Margin). *Palaeogeography, Palaeoclimatology, Palaeoecology* 231, 181–198.
- Hillenbrand, C.-D., Ehrmann, W., 2001. Distribution of clay minerals in drift sediments on the continental rise west of the Antarctic Peninsula, ODP Leg 178, Sites 1095 and 1096. In: Barker, P.F., Camerlenghi, A., Acton, G.D., Ramsay, A.T.S. (Eds.), *Proc. ODP, Sci. Results*, vol. 178, pp. 1–29 ((CD-ROM). Available from: Ocean Drilling Program, Texas A&M University, College Station TX 77845-9547, U.S.A.).
- Hillenbrand, C.D., Ehrmann, W., 2005. Late Neogene to Quaternary environmental changes in the Antarctic Peninsula region: evidence from drift sediments. *Global and Planetary Change* 45, 165–191.
- Hillenbrand, C.-D., Fütterer, D.K., 2002. Neogene to Quaternary deposition of opal on the continental rise west of the Antarctic Peninsula, ODP Leg 178, Sites 1095, 1096 and 1101. In: Barker, P.F., Camerlenghi, A., Acton, G.D., Ramsay, A.T.S. (Eds.), *Proc. ODP Sci. Results*, vol. 178, pp. 1–33 (CD-ROM). Available from: Ocean Drilling Program, Texas A&M University, College Station TX 77845-9547, U.S.A.
- Hillenbrand, C.-D., Camerlenghi, A., Cowan, E.A., Hernández-Molina, F.J., Lucchi, R.G., Rebesco, M., Uenzelmann-Neben, G., 2008. The present and past bottom-current flow regime around the sediment drifts on the continental rise west of the Antarctic Peninsula. *Marine Geology* 255, 55–63.
- Hodell, D.A., Venz, K., 1992. Toward a high-resolution stable isotopic record of the Southern Ocean during the Pliocene–Pleistocene (4.8 to 0.8 Ma). In: Kennett, J.D., Warnke, D.A. (Eds.), *The Antarctic paleoenvironment: a perspective on global change*. Antarct. Res. Ser., vol. 56. AGU, Washington, DC, pp. 265–310.
- Hofmann, E.E., Klinck, J.M., Lascara, C.M., Smith, D.A., 1996. Water mass distribution and circulation west of the Antarctic Peninsula and including Bransfield Strait. In: Ross, R.M., Hofmann, E.E., Quetin, L.B. (Eds.), *Foundations for Ecological Research West of the Antarctic Peninsula*. Antarctic Research Series, vol. 70. AGU, Washington, DC, pp. 61–80.
- Intergovernmental Panel on Climate Change (IPCC), report 2007: <http://www.ipcc.ch/>.
- Iwai, M., Acton, G.D., Lazarus, D., Osterman, L.E., Williams, T., 2002. Magnetobiochronology synthesis of ODP Leg 178 Rise Sediments from the Pacific sector of the Southern Ocean: Sites 1095, 1096 and 1101. In: Barker, P.F., Camerlenghi, A., Acton, G.D., Ramsay, A.T.S. (Eds.), *Proceeding ODP, Scientific Results, College Station (TX)*, pp. 1–40.
- Joseph, L.H., Rea, D.K., Van der Pluijm, B.A., Gleason, J.D., 2002. Antarctic environmental variability since the late Miocene: ODP Site 745, the East Kerguelen sediment drift. *Earth and Planetary Science Letters* 201, 127–142.
- Juntilla, J., Ruikka, M., Strand, K., 2005. Clay–mineral assemblages in high-resolution Plio-Pleistocene interval at ODP Site 1165, Prydz Bay, Antarctica. *Global and Planetary Change* 45, 151–163.
- Kennett, J.P., Hodell, D.A., 1995. Stability or instability of Antarctic ice sheets during warm climates of the Pliocene? *GSA Today* 5 (1), 9–22.
- Kirsch, H.J., 1991. Illite crystallinity: recommendations on sample preparation, X-ray diffraction settings, and interlaboratory samples. *J. Metamorph. Geol.* 9, 665–670.
- Krantz, 1991. *Quaternary Science Reviews* 10, 163–174.
- Lisiecki, L.E., Raymo, M.E., 2005. A Pliocene–Pleistocene stack of 57 globally distributed benthic $\delta^{18}O$ records. *Paleoceanography* 20, 1003.
- Lourens, L.J., Antonarakou, A., Hilgen, F.J., Van Hoof, A.A.M., Vergnaud-Grazzini, C., Zaccariasse, W.J., 1996. Evaluation of the Plio-Pleistocene astronomical Timescale. *Paleoceanography* 11, 391–413.
- Lucchi, R.G., Rebesco, M., 2007. Glacial contours on the Antarctic Peninsula margin: insight for palaeoenvironmental and palaeoclimatic conditions. In: Viana, A.R., Rebesco, M., Editors, *Economic and Palaeoceanographic Significance of Contourite Deposits*. Geol. Soc. London Special Publ. 276, 111–127.
- Lucchi, R.G., Rebesco, M., Camerlenghi, A., Busetti, M., Tomadin, L., Villa, G., Persico, D., Morigi, C., Bonci, M.C., Giorgetti, G., 2002. Mid-late Pleistocene glacial marine sedimentary processes of a high-latitude, deep-sea sediment drift (Antarctic Peninsula Pacific Margin). *Marine Geology* 189, 343–370.
- Martin, J.D., 2004. Qualitative and quantitative powder X-ray diffraction analysis.
- Müller, P., Schneider, R.R., 1993. An automated leaching method for the determination of opal in sediments and particulate matter. *Deep-Sea Research* 40, 425–444.
- Naish, T., Powell, R., Levy, R., Krissek, L., Niessen, F., Pompilio, M., Scherer, R., Talarico, F., Wilson, G., Wilson, T., Browne, G., Carter, C., Cody, R., Cowan, C., Crampton, J., Dunbar, G., Dunbar, N., Florindo, F., Gebhardt, C., Graham, I., Hannah, M., Harwood, D., Hansaraj, D., Henrys, S., Helling, D., Kuhn, G., Kyle, P., Läuffer, A., Maffioli, P., Mogens, D., Mandernack, K., McIntosh, W., McKay, R., Millan, C., Morin, R., Ohneiser, C., Paulsen, T., Persico, D., Reed, J., Ross, J., Raine, I., Schmitt, D., Sagnotti, L., Sjunneskog, C., Strong, P., Taviani, M., Vogel, S., Wilch, T., Williams, T., Winter, D., 2009. Late Cenozoic stability of the West Antarctic Ice Sheet. *Nature* 458, 322–328. doi:10.1038/nature07867. 19 March 2009.
- Nunes, R.A., Lennon, G.W., 1996. Physical oceanography of the Prydz Bay region of Antarctic waters. *Deep-Sea Research* 43 (5), 603–641.
- O'Brien, P.E., Cooper, A.K., Richter, C., et al., 2001. *Proc. ODP, Init. Repts.* 188 [Online]. Available from World Wide Web: http://www-odp.tamu.edu/publications/188_IR/188ir.htm.
- O'Brien, P.E., Cooper, A.K., Florindo, F., Handwerker, D., Lavelle, M., Passchier, S., Pospichal, J.J., Quilty, P.G., Richter, C., Theissen, K.M., Whitehead, J.M., 2004. Prydz channel fan and the history of extreme ice advances in Prydz Bay. In: Cooper, A.K., O'Brien, P.E., Richter, C. (Eds.), *Proc. ODP, Sci. Results*, vol. 188. [Online]. Available from World Wide Web: http://www-odp.tamu.edu/publications/188_SR/016/016-.
- Orsi, A.H., Whitworth III, T., Nowlin Jr., W.D., 1995. On the meridional extent and fronts of the Antarctic Circumpolar current. *Deep-Sea Research* 42 (5), 641–673.
- Passchier, S., 2007. Antarctic ice-sheet dynamics between 5.2 and 0 Ma from a high-resolution terrigenous particle size record, ODP Site 1165, Prydz Bay-Cooperation Sea. U.S. Geological Survey and The National Academies; USGS OF-2007-1047, Short Research Paper 043. doi:10.3133/of2007-1047.srp043.

- Passchier, S., O'Brien, P.E., Damuth, J.E., Januszczak, N., Handwerger, D.A., Whitehead, J.M., 2003. Pliocene–Pleistocene glaciomarine sedimentation in eastern Prydz Bay and development of the Prydz trough–mouth fan, ODP Sites 1166 and 1167, East Antarctica. *Marine Geology* 199, 179–305.
- Patterson, S.L., Whitworth III, T., 1990. Physical Oceanography. In: Glasby, G.P. (Ed.), *Antarctic Sector of the Pacific*. Elsevier Oceanographic Series, vol. 51. Elsevier, Amsterdam, pp. 55–93.
- Pickard, J., Adamson, D.A., Harwood, D.M., Miller, G.H., Quilty, P.G., Dell, R.G., 1988. Early Pliocene marine sediments, coastline, and climate of East Antarctica. *Geology* 16, 158–161.
- Pollard, D., DeConto, R.M., 2009. Modelling West Antarctic ice sheet growth and collapse through the past five million years. *Nature* 458, 329–332. doi:10.1038/nature07867. 19 March 2009.
- Pudsey, C.J., 2000. Sedimentation on the continental rise west of the Antarctic Peninsula over the last three glacial cycles. *Marine Geology* 167, 313–338.
- Pudsey, C.J., Camerlenghi, A., 1998. Glacial-interglacial deposition on a sediment drift on the Pacific margin of the Antarctic Peninsula. *Antarct. Sci.* 10, 286–308.
- Raymo, M.E., Grant, B., Horowitz, M., Rau, G.H., 1996. Mid-Pliocene warmth: stronger greenhouse and stronger conveyor. *Marine Micropaleontology* 27, 313–326.
- Rebesco, M., Larter, R.D., Barker, P.F., Camerlenghi, A., Vanneste, L.E., 1997. The history of sedimentation on the continental rise west of the Antarctic Peninsula. In: Barker, P.F., Cooper, A.K. (Eds.), *Geology and Seismic Stratigraphy of the Antarctic Margin, Part 2*. Antarctic Research Series, vol. 71. AGU, Washington DC, pp. 29–49.
- Rebesco, M., Camerlenghi, A., Volpi, V., Neagu, C., Accettella, D., Lindberg, B., Cova, A., Zgur, F., and the MAGICO Party, 2007. Interaction of processes and importance of contourites: insights from the detailed morphology of sediment drift 7, Antarctica. In: Viana, A.R., Rebesco, M. (Eds.), *Marine Economic and Palaeoceanographic Significance of Contourite Deposits*. Geol. Soc. London Special Publications 276, 95–110.
- Schrader, H.-J., Gersonde, R., 1978. Diatoms and silicoflagellates. In: Zachariasse, W.J., et al. (Ed.), *Micropaleontological counting methods and techniques – an exercise on an eight meter section of the Lower Pliocene of Capo Rosello, Sicily*: Utrecht Micropaleontological Bulletin, pp. 129–176.
- Shackleton, N.J., Crowhurst, S.J., Hagelberg, T., Pisias, N.G., Schneider, D.A., 1995. A new late Neogene time scale: application to Leg 138 sites. In: Pisias, N.G., Mayer, L.A., Janecek, T.R., Palmer-Julson, A., van Andel, T.H. (Eds.), *Proceedings of the Ocean Drilling Program. Scientific Results*, vol. 138. Ocean Drilling Program, College Station, TX.
- Skene, K.I., Piper, D.J.W., 2003. Late Quaternary stratigraphy of the Laurentian Fan: a record of events off the eastern Canadian continental margin during the last deglacial period. *Quaternary International* 99–100, 135–152.
- Sloan, L.C., Crowley, T.J., Pollard, D., 1996. Modeling of middle Pliocene climate with the NCAR GENESIS general circulation model. *Marine Micropaleontology* 27 (1/4), 51–61.
- Smellie, et al., 2009. *Earth Science Reviews* 94, 74–94.
- Smith, N.R., Zhaoqian, D.J., Kerry, K.R., Wright, S., 1984. Water masses and circulation in the region of Prydz Bay, Antarctica. *Deep-Sea Research Part A* 31, 1121–1147.
- Smith, D.A., Hofmann, E.E., Klinck, J.M., Lascara, C.M., 1999. Hydrography and circulation of the West Antarctic Peninsula Continental Shelf. *Deep-Sea Research* 46, 925–949.
- Stow, D.A.V., Faugères, J.C., 2008. Contourite facies and facies model. In: Rebesco, M., Camerlenghi, C. (Eds.), *Contourites: Development in Sedimentology*, vol. 60, pp. 223–250.
- Stow, D.A.V., Faugères, J.C., Gonthier, E., Cremer, M., Llave, E., Hernandez-Molina, F.J., Somoza, L., Diaz-Del-Rio, V., 2002. Faro-Albufeira drift complex, northern Gulf of Cadiz. In: Stow, D.A.V., Pudsey, C.J., Howe, J.A., Faugères, J.C., Viana, A.R. (Eds.), *Deep-water contourite systems: modern drifts and ancient series, seismic and sedimentary characteristics*: Geol. Soc. London Mem., vol. 22, pp. 137–154.
- Warnke, D.A., Richter, C., Florindo, F., Damuth, J.E., Balsam, W.L., Strand, K., Ruikka, M., Juntilla, J., Theissen, K., Quilty, P., 2004. Data Report: HiRISC (High-Resolution Integrated Stratigraphy Committee) Pliocene–Pleistocene interval, 0–50 mbsf at ODP Leg 188 site 1165, Bahia de Prydz, Antarctica. In: Cooper, A.K., O'Brien, P.E., Richter, C. (Eds.), *Proc. ODP Scientific Results*, pp. 1–38.
- Webb, P.-N., Harwood, D.M., 1991. Late Cenozoic glacial history of the Ross Embayment, Antarctica. *Quaternary Science Reviews* 10, 215–223.
- Webb, P.-N., Harwood, D.M., Mabin, M.G.C., McKelvey, B.C., 1996. A marine and terrestrial Sirius Group succession, middle Beardmore Glacier–Queen Alexandra Range, Transantarctic Mountains, Antarctica. *Marine Micropaleontology* 27 (1/4), 273–297.
- Whitehead, J.M., Bohaty, S.M., 2003. Pliocene summer sea-surface temperature reconstruction using silicoflagellates from Southern Ocean ODP Site 1165. *Paleoceanography* 18, 1075–1086.
- Whitehead, J.M., Quilty, P., Harwood, D.M., McMinn, A., 2001. Diatom palaeoenvironment of the Sorsdal Formation, Vestfold Hills based on diatom data. *Marine Micropaleontology* 41, 125–152.
- Whitehead, J.M., Wotherspoon, S., Bohaty, S.M., 2005. Minimal Antarctic sea ice during the Pliocene. *Geology* 33, 137–140.
- Zachos, J., Pagani, M., Sloan, L., Thomas, E., Billups, K., 2001. Trends, rhythms, and aberrations in global climate 65 Ma to present. *Science* 292, 686–693.
- Zielinski, U., Gersonde, R., 1998. Quaternary surface water temperature estimations: calibration of a diatom transfer function for the Southern Ocean. *Paleoceanography* 12 (4), 365–383.
- Zielinski, U., Gersonde, R., 2002. Plio/Pleistocene diatom biostratigraphy from ODP Leg 177, Atlantic sector of the Southern Ocean. *Marine Micropaleontology* 45, 225–268.